

**AFRL-RD-PS-
TP-2009-1007**

**AFRL-RD-PS-
TP-2009-1007**

**WAVELENGTH TUNING LIMITATIONS IN OPTICALLY
PUMPED TYPE-II ANTIMONIDE LASERS**

A.P. Ongstad et al.

7 January 2009

Journal Article

APPROVED FOR PUBLIC RELEASE; DISTRIBUTION UNLIMITED.



**AIR FORCE RESEARCH LABORATORY
Directed Energy Directorate
3550 Aberdeen Ave SE
AIR FORCE MATERIEL COMMAND
KIRTLAND AIR FORCE BASE, NM 87117-5776**

THIS PAGE INTENTIONALLY LEFT BLANK

REPORT DOCUMENTATION PAGE

Form Approved
OMB No. 0704-0188

Public reporting burden for this collection of information is estimated to average 1 hour per response, including the time for reviewing instructions, searching existing data sources, gathering and maintaining the data needed, and completing and reviewing this collection of information. Send comments regarding this burden estimate or any other aspect of this collection of information, including suggestions for reducing this burden to Department of Defense, Washington Headquarters Services, Directorate for Information Operations and Reports (0704-0188), 1215 Jefferson Davis Highway, Suite 1204, Arlington, VA 22202-4302. Respondents should be aware that notwithstanding any other provision of law, no person shall be subject to any penalty for failing to comply with a collection of information if it does not display a currently valid OMB control number. **PLEASE DO NOT RETURN YOUR FORM TO THE ABOVE ADDRESS.**

1. REPORT DATE (DD-MM-YYYY) 7-January-2009		2. REPORT TYPE Journal Article (Postprint)		3. DATES COVERED (From - To) 1-Jul-2007 - 1-Feb-2008	
4. TITLE AND SUBTITLE Wavelength Tuning Limitations in Optically Pumped Type-II Antimonide Lasers				5a. CONTRACT NUMBER In-House (DF297213)	
				5b. GRANT NUMBER	
				5c. PROGRAM ELEMENT NUMBER 62605F	
6. AUTHOR(S) A.P. Ongstad, R. Kaspi, G.C. Dente, M.L. Tilton*, J. Chavez*, R. Barresi*				5d. PROJECT NUMBER 4866	
				5e. TASK NUMBER LY	
				5f. WORK UNIT NUMBER 12	
7. PERFORMING ORGANIZATION NAME(S) AND ADDRESS(ES) Air Force Research Laboratory 3550 Aberdeen Avenue SE Kirtland AFB NM 87117-5776				8. PERFORMING ORGANIZATION REPORT NUMBER	
9. SPONSORING / MONITORING AGENCY NAME(S) AND ADDRESS(ES) AFRL/RDLAS 3550 Aberdeen Avenue SE Kirtland AFB NM 87117-5776				10. SPONSOR/MONITOR'S ACRONYM(S)	
				11. SPONSOR/MONITOR'S REPORT NUMBER(S) AFRL-RD-PS-TP-2009-1007	
12. DISTRIBUTION / AVAILABILITY STATEMENT Approved for public release; distribution is unlimited.					
13. SUPPLEMENTARY NOTES Published in Applied Physics Letters 92, 141106, (2008) American Institute of Physics GOVERNMENT PURPOSE RIGHTS					
14. ABSTRACT The authors examine the wavelength tuning limitations of type-II antimonide lasers containing In/As/InGaSb/InAs quantum wells. Wavelength running is accomplished by varying the thickness of the InAs electron wells while keeping all else fixed. In principle, these wells can be tuned from $\lambda \approx 2.5 \mu\text{m}$ out to far IR wavelengths by increasing the thickness of the InAs layers. However, a practical upper limit of $\lambda \approx 9.5 \mu\text{m}$ is set due to the high waveguide losses α_{wg} and the diminishing modal overlap with the gain at longer wavelengths.					
15. SUBJECT TERMS: Semiconductor lasers, optical pumping, type-II, free carrier absorbance, antimonide					
16. SECURITY CLASSIFICATION OF:			17. LIMITATION OF ABSTRACT	18. NUMBER OF PAGES	19a. NAME OF RESPONSIBLE PERSON Dr. Andrew Ongstad
a. REPORT Unclassified	b. ABSTRACT Unclassified	c. THIS PAGE Unclassified			Unlimited

Standard Form 298 (Rev. 8-98)
Prescribed by ANSI Std. Z39.18

Wavelength tuning limitations in optically pumped type-II antimonide lasers

A. P. Ongstad,^{1,a)} R. Kaspi,¹ G. C. Dente,² M. L. Tilton,² R. Barresi,² and J. R. Chavez²

¹*Air Force Research Laboratory, Directed Energy Directorate, Kirtland AFB, Albuquerque, New Mexico 87117, USA*

²*Boeing Defense and Space Group, Albuquerque, New Mexico 87106, USA*

(Received 26 February 2008; accepted 11 March 2008; published online 8 April 2008)

In this paper, we examine the wavelength tuning limitations of type-II antimonide lasers containing InAs/InGaSb/InAs quantum wells. Wavelength tuning is accomplished by varying the thickness of the InAs electron wells while keeping all else fixed. In principle, these wells can be tuned from $\lambda \approx 2.5 \mu\text{m}$ out to far IR wavelengths by increasing the thickness of the InAs layers. However, a practical upper limit of $\lambda \approx 9.5 \mu\text{m}$ is set due to the high waveguide losses a_{wg} and the diminishing modal overlap with the gain at longer wavelengths. The waveguide losses grow as $a_{\text{wg}} \propto \lambda^{3.44}$ and are attributable to free carrier absorbance. In order for the long-IR laser devices to achieve threshold, they must continually band fill, spectrally tuning to shorter wavelengths, until the laser gain exceeds the losses, which occurs near $9.5 \mu\text{m}$. © 2008 American Institute of Physics.

[DOI: 10.1063/1.2904702]

Many applications, including remote chemical sensing as well as infrared countermeasures (IRCM) require lasers that operate in the 2–10 μm wavelength range. This wavelength region is important. Several atmospheric transmission windows are suitable for IRCM applications. This region also constitutes the fingerprint region of molecular absorbance, where pumping of molecular vibrational transitions can lead to highly sensitive spectroscopic detection methods. Clearly, it would be advantageous to use a single semiconductor material system and quantum well laser design to provide cw laser sources to cover this entire region. Indeed, the antimonide based III-V compounds can be used in this capacity. We employ 14 type-II InAs/InGaSb/InAs quantum wells which are imbedded in thick 1000 Å lattice-matched quaternary (InGaAsSb) layers. The InGaSb layer provides a well for holes and is typically fixed at 8 ML thickness. The InAs layers then provide coupled quantum wells for electrons. Wavelength tuning in this broken-gap band alignment is accomplished by increasing the width of the InAs electron wells, which effectively lowers the energy of the trapped electronic state such that the emission moves to longer wavelengths. The thickness of the other epitaxial layers is normally not changed. Laser devices were grown in our laboratory using a commercial solid-source molecular beam epitaxial chamber specifically configured for antimonide alloy growth.¹ A representative type-II well is shown as an inset in Fig. 1.

The epitaxial material was processed into 2.5 mm long edge emitting lasers, which were then optically pumped by a high-power 1.85 μm laser diode array. The thick quaternary regions absorb a majority of the pump radiation. The photo-generated carriers then transport from the quaternary layer into the type-II wells, providing the optical gain.

In this paper, we examine the practical wavelength tuning limitations of this epitaxial system. Figure 1 plots the emission wavelength versus the InAs layer thickness in monolayers for a large set of W lasers. The graph also shows

the theoretical wavelength tuning curve calculated by a superlattice pseudopotential model (SEPM).^{2–4}

When the InAs electron quantum well thickness is set to its minimum value of 1 ML ($\approx 3 \text{ \AA}$), the resulting low wavelength limit is near 2.5 μm . Interestingly, if the electron well is completely eliminated (i.e., 0 ML InAs), the emission wavelength of the resulting epitaxy falls to $\sim 2.3 \mu\text{m}$.

As is evident in Fig. 1, the emission wavelength of the W wells can be tuned to very long wavelengths by appropriately increasing the thickness of the InAs layers. For example, the SEPM calculations indicate the emission wavelength for W lasers with 10 and 13 ML of InAs would be near 10 and 20 μm , respectively. However, Fig. 1 shows that for devices with average InAs layer thickness of 9.6, 11.2, and 12.4 ML the lasing emission did not exceed $\sim 9.5 \mu\text{m}$. Figure 1 shows excellent agreement between the measured laser wavelengths and the SEPM calculations for InAs layer thicknesses below about 7 ML, i.e., $\lambda < 6 \mu\text{m}$, but shows

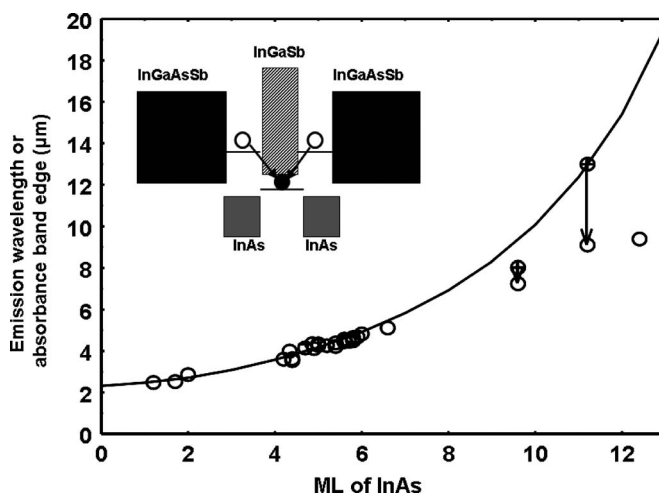


FIG. 1. Experimental results and SEPM calculated tuning curve for the wavelength at the subband edge vs InAs layer thickness. The circles are the laser measured wavelengths for devices with quaternary concentrations of 20% indium. The symbols with crosses are the band-edge energies determined from FTIR absorbance measurements. The inset shows a representative W quantum well.

^{a)}Electronic mail: andrew.ongstad@kirtland.af.mil.

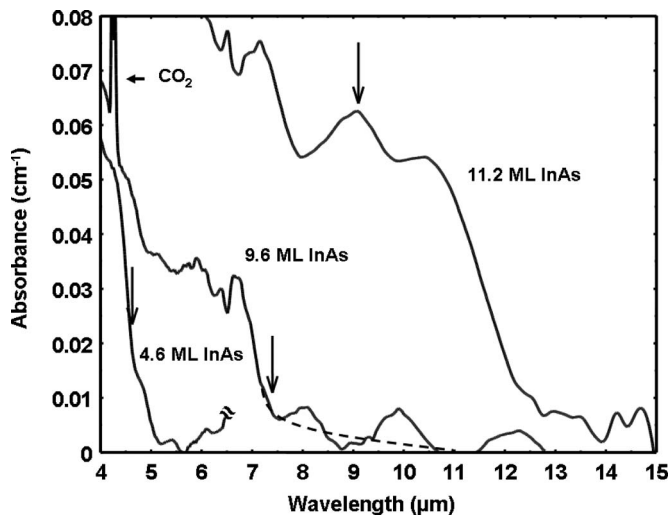


FIG. 2. The absorbance spectra for devices with average InAs layer thickness of 4.6, 9.6, and 11.2 ML. The dotted curve is the projected absorbance tail with the etaloning removed. The arrows mark the points at which laser emission was observed. The 4.6 ML laser device had a higher quaternary concentration of 25% indium, for clarity its absorbance is clipped at $6.5 \mu\text{m}$.

increasing deviation above that point as the InAs layer thickness is increased.

The laser emission wavelength shift to higher energies is suggestive of band filling. To assess the location of the fundamental subband edge, the laser samples were optically characterized by absorbance measurements using a Nicolet Magna 760 Fourier transform IR (FTIR) spectrometer in the transmission mode. The laser samples were mounted using copper adhesive tape over an aperture in the cold finger of a liquid-nitrogen-cooled cryostat. The absorption spectra from the samples were first normalized with respect to window transmission and system response at the time of collection. In addition, substrate-related absorption features were eliminated by subtracting an absorption spectrum of the bare substrate from the laser sample spectrum. The resulting set of absorption spectra from three laser samples with 4.7, 9.6, and 11.2 ML are shown in Fig. 2. In general, the absorption spectra are quite clean, exhibiting a relatively sharp band edge for the transition from the first conduction subband to the first valence subband. However, a sinusoidal baseline ripple appears in the spectrum of the 4.6 and 9.6 ML laser samples. This etaloning is due to the small index step, $\Delta n \sim 0.04$, between the well region and the substrate. The period of the modulation of $\approx 214 \text{ cm}^{-1}$ yields a layer thickness of $6.15 \mu\text{m}$ for the sample, which favorably compares with $6.08 \mu\text{m}$ for the as-grown structure.

For the laser device with 4.7 ML of InAs, the laser emission wavelength assessed at the half maximum intensity point on the low energy side is very close to the observed absorbance subband edge, as can be seen in Fig. 2. In contrast, the other spectra show absorbance band edges further removed from the laser line. For example, for the devices with 9.6 and 11.2 ML of InAs, the absorption band edges are near 8 and $13 \mu\text{m}$, respectively.

Figure 3 shows a plot of the absorbance coefficient ϵ for a compensated GaSb substrate on which our W laser were grown. Since the GaSb boule is intrinsically *p* type it is compensated with $(1-3) \times 10^{17} \text{ cm}^{-3}$ of tellurium resulting in an *n*-type material. The compensated doping is intended to reduce free-carrier absorbance at 77 K. For the absorbance

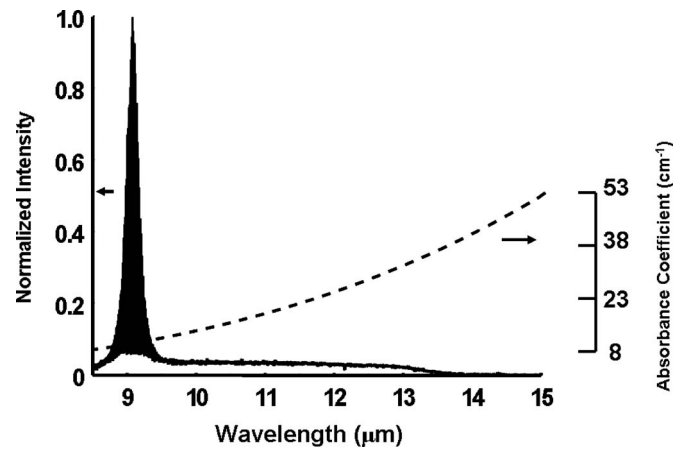


FIG. 3. Right side: the absorbance coefficient for a *n*-doped GaSb substrate as a function of wavelength. The dashed line is a fit to $\epsilon = a \times \lambda^b$ where $a = 0.0049$ and $b = 3.44$. Left side: a subthreshold spectrum for the device with 11.2 ML of InAs. Note the density-of-states like intensity step beginning near $13.5 \mu\text{m}$ and remaining clamped until approximately $9.5 \mu\text{m}$ at which point laser amplified spontaneous emission begins.

measurement at 78 K, the epitaxy was removed by lapping off $\sim 10 \mu\text{m}$ of material on the epitaxial side of the chip and then polishing it to a mirrorlike finish. The absorbance spectrum is characterized by a monotonic structureless spectrum which grows as $\lambda^{3.44}$. This is characteristic of free-carrier absorbance in which the $\lambda^{3.44}$ dependence is attributable to scattering by the ionized dopant.⁵

For the W lasers, the GaSb absorbance coefficient will closely approximate the lasers waveguide loss a_{wg} . This is due to the fact that the W-active region clad layers are GaSb and provide for extremely weak index guiding of the transverse mode. In fact, the index step between the superlattice and the GaSb clad is estimated to be only $\Delta n \approx 0.04$. Employing a complex dielectric waveguide model, we calculated the modal intensity as a function of wavelength for W lasers operating from 5 to $11 \mu\text{m}$. The results, displayed in Fig. 4, show that the optical mode extends anywhere from $10-50 \mu\text{m}$ into the substrate with the longer wavelength devices showing longer modal tails. Since a significant fraction of the mode samples the GaSb substrate $a_{\text{wg}} \sim \epsilon_{\text{GaSb}}$. This

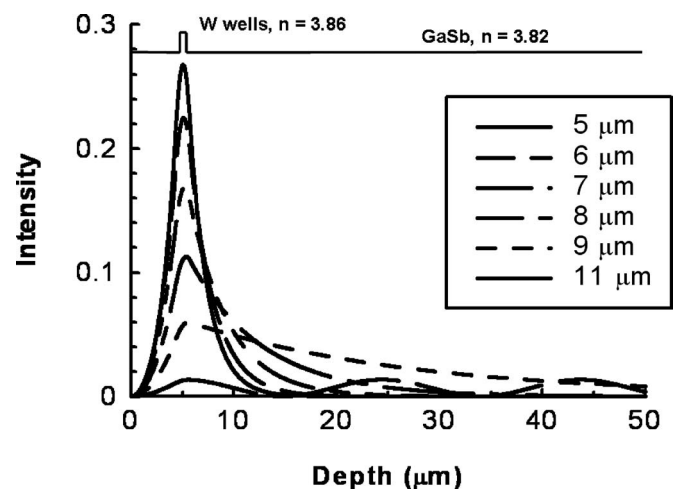


FIG. 4. A plot of the transverse modal intensity for different wavelength devices vs depth through the structure. The upper line shows the index step and position of the quantum wells for the baseline W laser structures employed in this study.

suggests that the waveguide losses for the long-IR W lasers are appreciable. From the GaSb absorbance data (see Fig. 3), the estimated losses near the band-edge energies for the lasers containing 9.6 and 11.2 ML InAs are 6.2 and 33 cm^{-1} , respectively. For the device with 12.4 ML InAs and a SEPM band-edge calculated at $17\text{ }\mu\text{m}$, the extrapolated loss is very large at 99 cm^{-1} . For comparison the mirror outcoupling losses were 4.3 cm^{-1} for the devices under test which were 2.5 mm in length with uncoated facets. For wavelengths below $\approx 5\text{ }\mu\text{m}$ the losses are considerably less ($a_{\text{wg}} \leq 2\text{ cm}^{-1}$). Indeed, the low a_{wg} predicted for the shorter wavelength devices are supported by waveguide loss measurements done by a Hakki–Paoli “in-the-bandgap” measurement,⁶ as well as by the more traditional study in which the laser differential quantum efficiency is measured as a function of cavity length. For the laser with 4.7 ML of InAs, $\lambda_{\text{lase}}=4.62$, the measured loss value, as determined by an average of the two techniques, was 1.5 cm^{-1} .

Two factors then serve to limit the long wavelength operation of these W lasers, the rapidly rising waveguide loss with increasing wavelength and the reduced modal overlap with the gain as wavelength increases. Certainly, the large waveguide losses may greatly exceed the maximum small-signal gain coefficient g given by $g = \Gamma \times g_{\text{SL}}$, where Γ is the modal overlap and g_{SL} is the superlattice material gain. In order to reach threshold, the small-signal gain must exceed the sum of waveguide plus mirror losses. For the laser structure with 11.2 ML of InAs to reach threshold at $\lambda = 13\text{ }\mu\text{m}$ would require $\approx 37\text{ cm}^{-1}$ of gain. Since the maximum small-signal gain is considerably below this value, the device must band fill in order to reach the point at which the gain equals the losses. In fact, it must spectrally tune to shorter wavelengths by continually band filling until the gain exceeds the losses. Such a process is evident in the subthreshold FTIR spectrum shown in Fig. 3. In this spectrum, a clear low-intensity step is observed near $13.5\text{ }\mu\text{m}$ which stays nearly constant in intensity until a sharp increase in amplified spontaneous emission is seen, beginning at $\sim 9.5\text{ }\mu\text{m}$ and peaking at $9.1\text{ }\mu\text{m}$. We note that the constant intensity step beginning near $13.5\text{ }\mu\text{m}$ remarkably appears like a density-of-state function for the first energy state in a quantum well. Other mechanisms, which shift the lasing wavelength from the sub-band edge, have been observed in type-II GaAsSb lasers.

These “blueshift” mechanisms include charge separation, band distortion, and many-body interactions.⁷

The results of this investigation suggest that the upper wavelength limit may be extended somewhat beyond $\approx 9.5\text{ }\mu\text{m}$ by employing a waveguide with a larger Γ value. The current low Γ , or dilute waveguide design, for these W lasers was chosen in order to decrease the transverse divergence while simultaneously suppressing filament formation in the resonator. The dilute waveguide design has been extremely capable in this regard with a low transverse divergence of $\approx 22^\circ$ and a small antiguiding factor < 1 . However, such a design is not as efficient in adequately confining the transverse mode in a device operating beyond $\sim 9.5\text{ }\mu\text{m}$. Furthermore, the rapidly increasing waveguide losses indicate that even though the InAs/InGaSb/InAs epitaxy can in principle be tuned to extremely long wavelengths, the large waveguide losses will place a practical upper limit of operation independent of the waveguide design.

In summary, we have investigated the wavelength tuning limitations of type-II antimonide based heterostructures. The low wavelength limit is near $2.5\text{ }\mu\text{m}$ and is set by the minimum InAs layer thickness of 1 ML. SEPM theory predictions indicate these devices can be tuned to very long wavelengths by increasing the thickness of the InAs electron wells. However, FTIR absorbance measurements reveal that the rapidly increasing waveguide loss growing as $\lambda^{3.44}$, as well as the diminishing modal overlap with the gain places a practical upper wavelength limit of $\lambda_{\text{lase}} \leq 9.5\text{ }\mu\text{m}$ on devices with thick InAs layers. The absorbance measurements have shown that for these devices to reach threshold, they must band fill, thereby moving down the free-carrier loss curve, until the gain equals the loss.

¹R. Kaspi, A. P. Ongstad, G. C. Dente, J. R. Chavez, M. L. Tilton, and D. M. Gianardi, *Appl. Phys. Lett.* **88**, 041122 (2006).

²G. C. Dente, M. L. Tilton, A. P. Ongstad, and R. Kaspi, *J. Appl. Phys.* **103**, 023106 (2008).

³G. C. Dente and M. L. Tilton, *J. Appl. Phys.* **86**, 1420 (1999).

⁴G. C. Dente and M. L. Tilton, *Phys. Rev. B* **66**, 165307 (2002).

⁵J. I. Pankove, *Optical Processes in Semiconductors* (Dover, New York, 1971).

⁶S. Suchalkin, D. Westerfeld, D. Donetsik, S. Luryi, G. Belenky, R. Martinelli, I. Vurgaftman, and J. Meyer, *Appl. Phys. Lett.* **80**, 2833 (2002).

⁷W. W. Chow, O. B. Spahn, H. C. Schneider, and J. F. Klem, *IEEE J. Quantum Electron.* **37**, 1178 (2001).